RSC Advances

PAPER

View Article Online
View Journal | View Issue

Cite this: *RSC Adv.*, 2020, **10**, 21517

Electrochemical studies of prothioconazole as a novel corrosion inhibitor for copper in acidic solutions

Zhihua Tao, †*[a] Yuanxun Li, †*[bc] Yi Xiao Peng,[a] Hua Su,[b] Likun Han[b] and Guanting Liu[a]

Received 31st March 2020
Accepted 7th May 2020

DOI: 10.1039/d0ra02919j

rsc.li/rsc-advances

Prothioconazole is a fungicide that has a wide number of applications in agriculture, and it can ensure the safety of crops, users, and the environment. Prothioconazole, as a suppressor of copper dissolution in 0.5 M H_2SO_4 solution, has been evaluated using electrochemical experiments, weight loss tests, quantum chemical calculations, and scanning electron microscopy (SEM). The electrochemical test results showed that prothioconazole was an excellent inhibitor, and the anticorrosion ability increased with the inhibitor concentration. The interaction of prothioconazole with copper is a spontaneous adsorption process accompanied by typical chemisorption. The number of water molecules (*X*) displaced by one prothioconazole molecule was obtained using diverse substitutional adsorption models based on electrochemical impedance spectroscopy (EIS) data. In addition, the Fukui functions indicate that the triazole and benzene rings and the –C=S atoms were the main active sites for the adsorption process.

1. Introduction

Copper and copper alloys with their high-strength and high-conductivity, are widely used in the printed circuit board (PCB) manufacturing industry, as integrated circuit (IC) packaging materials, signal shielding devices, electrical pick-off contact supports and contact materials, joining Cu dissimilar joints using soldering and so on.[1–3] Using electroless plating copper or the electroplate process on double-sided printed circuit boards (PCBs) or multi-layers rigid-flex PCBs, some metals can be deposited on the dielectric surface of polyimide (PI) or epoxy resin (EP) materials. The layer of metal can achieve interconnection of the double sided circuit.[4,5] For electrodeposition, the cleaning of rusty spots and grease is an important part of the pre-plating process for the copper material surfaces. Cu has the disadvantage that it is easily corroded in acidic solution, this can be prevented by adding some organic compounds (anti-corrosion inhibitor) as a relatively simple and practical approach.[6–9] Classically, the functional groups of numerous anti-corrosion inhibitors containing heterocyclic compounds, such as thiol, nitrogen and oxygen, for example benzotriazole (BTA) and its derivatives, are effective and normal inhibitors that are used for the anticorrosion of copper and its alloys in industry. However, the problem with BTA is the toxicity and poor solubility in water. Prothioconazole is a broad-spectrum organic fungicide that has been efficiently and widely used in disease prevention and control for cotton, beans, tomatoes, cereals and wheat crops. Propanthiazole has a better biological activity, no teratogenicity and is safe for humans and the environment.[10] In addition, propanthiazole has an excellent water-solubility and biodegradability compared with benzotriazole derivatives.[11,12] Fortunately, the processes for preparing propanthiazole has some advantages, such as less extensive raw materials, easily recycled reaction solvents, milder conditions, and a high product quality.[13–15] Given the circumstances, using propanthiazole as an organic inhibitor reduces the labor intensity and pollution, and conserves water resources. To the best of our knowledge, prothioconazole as an anti-corrosion agent for copper in acidic solution has not been explored previously by scholars. Hence, in the present study, the inhibiting performance and anticorrosion mechanism of prothioconazole were investigated using traditional methods such as electrochemical experiments, weight loss tests, quantum chemical calculations and scanning electron microscopy (SEM) analysis.

[a]*Department of Applied Chemistry, School of Materials and Energy, University of Electronic Science and Technology of China (UESTC), Chengdu, 610054, China. E-mail: Tzh3595@uestc.edu.cn*

[b]*State Key Lab of Electronic Thin Films and Integrated Devices, University of Electronic Science and Technology of China (UESTC), Chengdu, 610054, China. E-mail: Liyuanxun@uestc.edu.cn*

[c]*Dongguan Chengqi Cichuang Innovation Materials Co., Ltd, Dongguan, 523808, China*

† Zhihua Tao and Yuanxun Li contributed equally to this work.

2. Experimental

2.1. Materials and sample preparation

The studied inhibitor, prothioconazole (2-(2-(1-chlorocyclopropyl)-3-(2-chlorophenyl)-2-hydroxypropyl)-1*H*-1,2,4-

triazole-3(2*H*)-thione), was synthesized *via* a Grignard reaction using substituted hydrazines, and cyclization and oxidation reactions.[15,16] Prothioconazole is a yellow solid, with a melting point of 138–139 °C, and a yield of 93.0%, the synthesis route for prothioconazole and its molecular structures is shown in Fig. 1. The prothioconazole used in the corrosion experiment was purchased from Shanghai Boka Chemical Technology Co., Ltd. The base erosion solution consists mainly of 0.5 M H_2SO_4. The 0.5 M H_2SO_4 solution (300 mL) used for corrosion testing was established by dilution of sulfuric acid (98%) with distilled water. The range of test concentrations of prothioconazole are 5×10^{-6} to 10^{-4} mol L^{-1} in 0.5 M H_2SO_4 solution. In the absence of prothioconazole the solution is considered to be a blank and is used for comparison.

2.2. Electrochemical tests

The inhibiting performance of prothioconazole on a Cu electrode surface was analyzed using an electrochemical workstation (CHI760E Instrument) with a 500 mL capacity for a three-electrode system. The Cu electrode specimens were immersed in 300 mL of erosion solution with and without the addition of different concentrations of prothioconazole at 288, 298, 308 and 318 K, respectively. A platinum (Pt) electrode with a 2 cm length on one side of the square and a red copper bar (99.999%) with a diameter of 1.0 cm were adopted as the counter electrode and the test Cu electrode, respectively. A saturated mercurous sulfate electrode (SMSE), which was used as the reference electrode, was placed in a small Teflon tube that contained the blank solution. The erosion solution was in contact with the air and various kinds of electrochemical measurements were carried out in a thermostat water bath, and the temperatures of the test solution were controlled accurately using advanced digital thermostat control technology. All potentials measurements were carried out on the Cu electrode with reference to the SMSE.

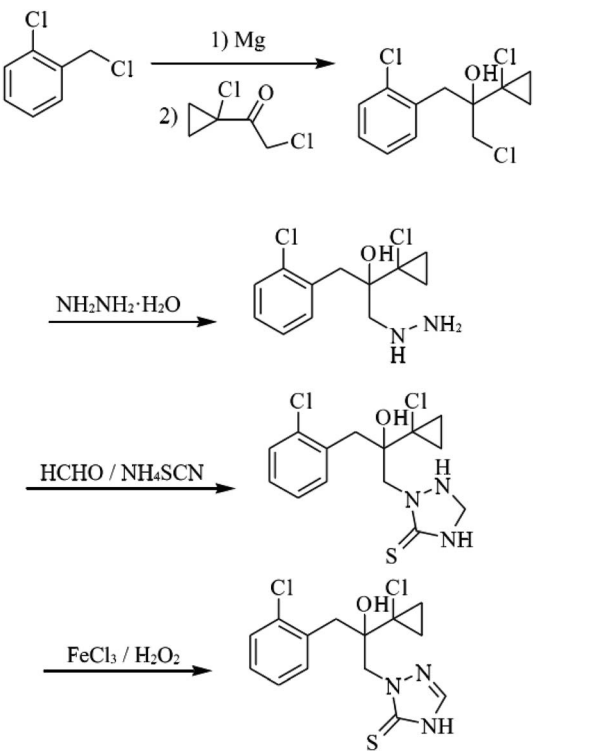

Fig. 1 The synthetic routes to prothioconazole.

Prior to the measurement, the test Cu electrode was packaged in epoxy resin with a 1.0 cm diameter geometrical surface area exposed to the electrolyte. The surface of the test Cu electrodes was polished to restore the shine using emery paper, the electrodes were then chemically degreased for pre-processing and then rinsed with distilled water. The degreased working electrodes were dried at room temperature and then those used as the working electrodes were inserted into the solution.

Tafel polarization measurements were carried out from −0.25 to +0.25 V (*vs.* open-circuit potential (OCP)) with a 1 mV s^{-1} scanning rate of potential at differing temperatures (288–318 K). The electrochemical impedance spectroscopy (EIS) data were acquired in the frequency range from 100 kHz to 0.01 Hz at a steady-state OCP. A 10 mV peak-to-peak sine wave was considered to be a potential perturbation signal.

2.3. Surface analysis and weight loss tests

To analyze the corrosive morphology and adsorption mechanics of Cu during corrosion processing better, an immersion test for the pure Cu was carried out. The copper coupons (99.9%) were cut to the desired dimensions of 3.0 × 1.5 × 1.5 cm for SEM analysis and the weight loss test. The conditions of the soaking temperature, soaking time, and the size of the samples were determined, and the samples were soaked in 0.5 M H_2SO_4 at a temperature of 308 K for 8 h. After the weight loss test, the copper block was removed from the 500 mL glass cell and rinsed with a high-pressure water washing device and then dried at room temperature. The Cu sample thickness and weight loss had changed after the immersion test. The weight loss test data were obtained from the average value of three parallel Cu samples in the erosion solution with different concentrations of prothioconazole. The corrosion metal surface morphology and microstructure were observed and investigated using a Hitachi SU3500 SEM instrument.

2.4. Quantum chemical calculations

On the basis of the quantum chemical calculation,[16] the structural–property parameters were further analyzed using the DMol3 module according to density functional theory (DFT). The prothioconazole compound was fully geometrically optimized using the GGA/BLYP method with a double numerical plus polarization (DNP) basis set. The solvent effects on the geometric and electronic properties of the prothioconazole compound were further considered according to the conductor-like screening model (COSMO).

3. Results and discussion

3.1. Polarization curve tests

The key corrosion parameters based on the electrochemical behavior were studied using the measurement of the

potentiodynamic polarization curves at different temperatures and concentrations. It can be clearly seen from the potentiodynamic polarization experiments (as shown in Fig. 2) that the anticorrosive effects are strengthened with the increasing concentration of prothioconazole. To study the influences of the different temperature conditions (288–318 K) on the corrosive media, the electrochemical etching parameters of the corrosion potential (E_{corr}), the anodic slopes (β_a), corrosion current density (I_{corr}), and the cathodic slopes (β_c) based on the potentiodynamic Tafel test are listed in Table 1. The inhibitive efficiency at different temperatures and inhibitor concentrations was calculated according to the following equation:[13,14]

$$I_{EI}\% = \frac{I_{blank} - I_{inh}}{I_{blank}} \times 100 \quad (1)$$

The corrosion parameters of I_{blank} and I_{inh} represent the current density without prothioconazole and those with various concentrations of prothioconazole in the etching solutions, respectively. The corrosion current density showed a declining trend along with the rapidly increasing concentration of prothioconazole in the etching solution, in other words, the activity of corrosion was inhibited when prothioconazole was mixed in a solution of sulphuric acid. Therefore, the key corrosion parameters of $I_{corr(inh)}$ lead to an increase in the inhibition efficiencies, up to their maximum values of 97.7%, 93.9%, 94.9% and 98.1% for 288, 298, 308 and 318 K respectively. When prothioconazole was added to the solution, the corrosion potential of E_{corr} shifted towards the positive and the cathodic curve was roughly parallel to the inhibitor-free cathodic curve, this phenomenon could be attributed to fact that the hydrogen evolution has better activity control and the corrosion mechanism is not affected by prothioconazole.[17,18] Considering that the difference in the corrosion potential between the minimum and maximum values was less than 85 mV at the same temperature, prothioconazole can be classified as a mixed-type inhibitor.[19,20] The data for the Tafel slopes of the anodic and cathodic (β_a, β_c) reactions changed little under the different inhibitor concentrations, suggesting that the prothioconazole adsorption on the metal surface blocked both the cathodic and anodic corrosion reactions and that prothioconazole has little effect on the metal dissolution mechanism (cathodic hydrogen evolution).[21] The temperature is one of the most important parameters in the acid scrubbing process. Cu metal has a high corrosion current density in corrosive media without an inhibitor, as shown in Table 1. It can also be seen that prothioconazole has an excellent inhibition efficiency against corrosion in corrosive media in the 288–318 K temperature range.

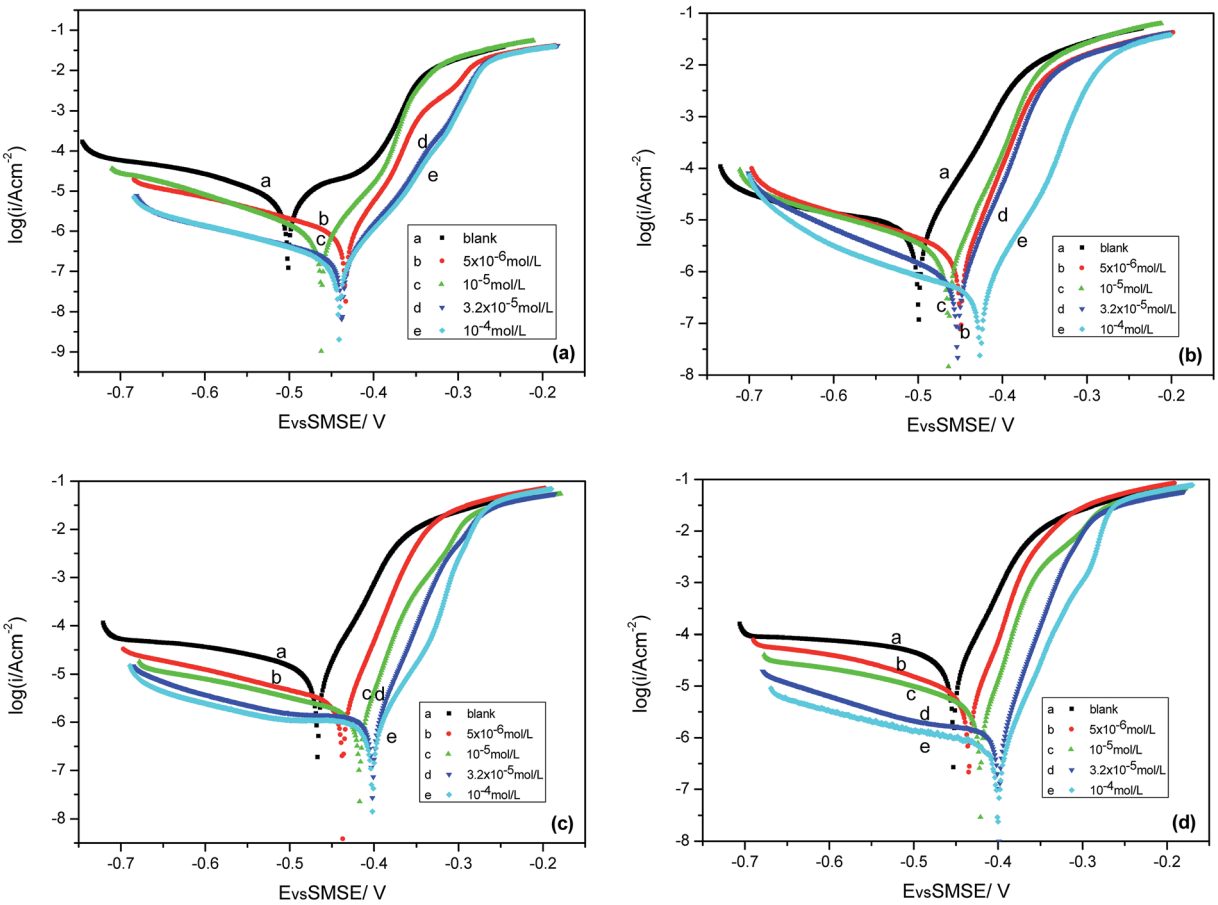

Fig. 2 Polarization curves for copper in 0.5 M H_2SO_4 solution containing various concentrations of prothioconazole: (a) 288; (b) 298; (c) 308; and (d) 318 K.

Table 1 Tafel corrosion parameters for copper in acidic solution with different concentrations of prothioconazole

Temperature (K)	Concentration (M)	E_{corr} (mV *vs.* SMSE)	β_c (mV dec^{-1})	β_a (mV dec^{-1})	I_{corr} (μA cm^{-2})	I_{EI}%
288	Blank	−501	169.9	58.4	6.16	—
	5×10^{-6}	−433	174.8	35.1	0.85	86.2
	10^{-5}	−462	141.0	20.8	0.41	93.3
	3.2×10^{-5}	−438	195.5	31.8	0.18	97.1
	10^{-4}	−441	179.1	33.0	0.14	97.7
298	Blank	−499	296.9	35.8	5.58	—
	5×10^{-6}	−450	206.0	40.7	2.56	54.1
	10^{-5}	−464	204.1	30.3	1.78	68.1
	3.2×10^{-5}	−453	156.3	30.2	0.69	87.6
	10^{-4}	−426	195.4	25.6	0.34	93.9
308	Blank	−467	285.4	42.8	11.82	—
	5×10^{-6}	−437	231.1	38.0	3.27	72.3
	10^{-5}	−417	235.7	40.1	2.05	82.7
	3.2×10^{-5}	−402	130.7	35.2	1.50	87.3
	10^{-4}	−402	135.1	21.3	0.60	94.9
318	Blank	−453	317.5	55.4	37.26	—
	5×10^{-6}	−435	200.0	51.3	9.10	75.6
	10^{-5}	−421	230.8	64.4	6.77	81.8
	3.2×10^{-5}	−399	355.2	35.4	1.78	95.2
	10^{-4}	−400	353.1	33.4	0.71	98.1

3.2. Electrochemical impedance spectroscopy

The effects of the alternating-current (AC) impedance technique on the Cu surface properties and the kinetics of the electrode processes were studied. The relevant Nyquist plots for the copper electrode in 0.5 M H_2SO_4 erosion solution with different concentrations of prothioconazole are shown in Fig. 3. The

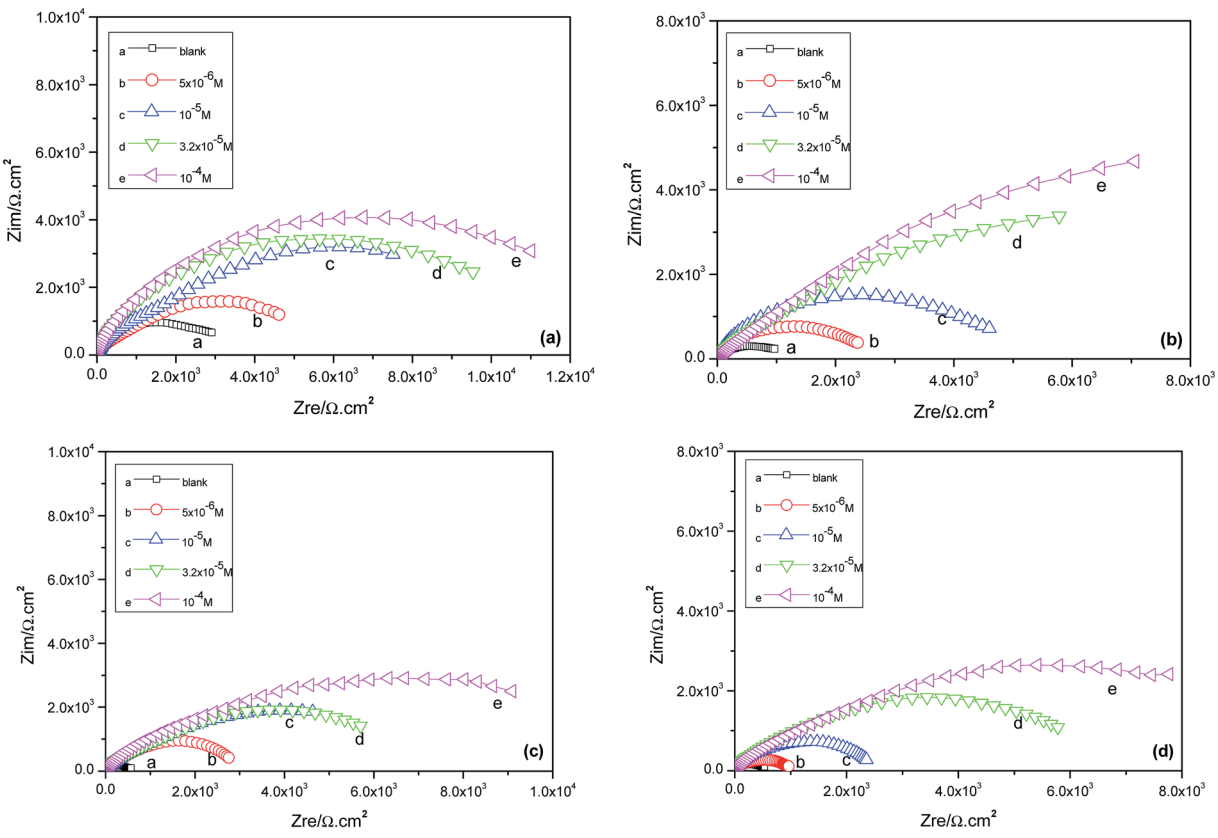

Fig. 3 Nyquist plots for copper in 0.5 M H_2SO_4 solution containing different concentrations of prothioconazole: (a) 288; (b) 298; (c) 308; and (d) 318 K.

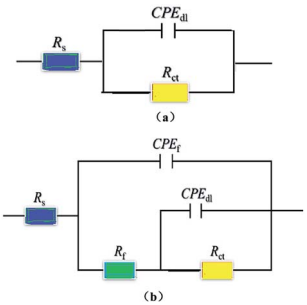

Fig. 4 The equivalent circuit model used to fit the EIS data for copper in acidic solution: (a) equivalent circuits of (R(QR)) and (b) equivalent circuits of R(Q(R(QR))).

diameter of the capacitive arcs showed a strengthening trend in comparison with that obtained from the corroded copper in the inhibitor-free solution, which illustrates the better inhibition performance of the prothioconazole base and its strong adsorption ability on the material surface.[16] According to Fig. 3, we know that the Nyquist plots reveal suppressed semicircles and the deviation change from the ideal semicircular arc, this phenomenon is often attributed to the frequency dispersion characteristics of the real interfacial impedance.[22–24] The change in the principles of the electrochemical impedance *versus* the temperature or concentration of prothioconazole was analyzed by simulating the experimental data using an appropriate equivalent circuit.[25,26] In this paper, two general equivalent circuits for the impedance data were proposed and are shown in Fig. 4. The Nyquist curve containing a single capacitance arc for Cu in the erosion solution was analyzed using a standard Randles circuit model as shown in Fig. 4a. Accordingly, the analytical calculations of the impedance spectra with the film capacitance (CPE_f) are presented systematically in Fig. 4b. As presented in Fig. 4, R_s is the solution resistance, R_f represents the resistance of the adsorption film resistance, R_{ct} is the resistance ascribed to the charge transfer resistance, and the analysis of the CPE_{dl} and CPE_f values was used as the constant phase elements (CPE). In addition, the CPE_f is made up of the film capacitance Y_f and the deviation parameter n_f, the CPE_{dl} is formed with a double-layer capacitance Y_{dl} and the deviation parameter n_{dl}. The constant phase elements are described using the expression:[27,28]

$$Z_{CPE} = Y^{-1}(j\omega)^{-n} \quad (2)$$

In which Y represents the main body of the CPE, j is a symbol for recording the imaginary unit, omega (ω) represents the angular frequency ($2\pi f$) and the deviation parameter n has been defined to estimate the nature of the microcosmic interfaces of Cu and reflects microscopic fluctuations on the surface. If $n = 0$, the CPE is identical to a pure resistor, and for $n = 1$, a pure capacitor. It was easy to analyze the corrosion inhibitor efficiency of the prothioconazole base on the charge transfer resistance of EIS data by using the formula:[29]

$$I_{EZ}\% = \frac{R_{ct} - R_{ct}^0}{R_{ct}} \times 100 \quad (3)$$

In which R_{ct}^0 and R_{ct} represent the electron-transfer resistance of the electrode/electrolyte interface in the absence and presence of prothioconazole in acidic solution, respectively. Furthermore, the CPE parameter values Y and n for calculating the C_{dl} (double layer capacitance) were established using the following equation:[16]

$$C_{dl} = \frac{Y\omega^{n-1}}{\sin(n(\pi/2))} \quad (4)$$

Table 2 Fitting analysis of the EIS spectra for copper in acidic solution with different concentrations of prothioconazole

				CPE_f			CPE_{dl}		
Temperature (K)	Concentration (M)	R_s (Ω cm^2)	R_f (Ω cm^2)	Y_f (μF cm^{-2})	n_1	R_{ct} (Ω cm^2)	Y_{dl} (μF cm^{-2})	n_2	I_{EZ}%
288	Blank	1.9	—	—	—	2723.0	41.8	0.85	—
	5×10^{-6}	1.8	1204	24.3	0.77	4587	86.7	0.64	40.6
	10^{-5}	3.1	2637	23.5	0.80	8594	89.5	0.69	68.3
	3.2×10^{-5}	2.0	1796	13.4	0.90	10 440	42.7	0.54	73.9
	10^{-4}	2.0	63.4	9.8	0.92	15 220	33.6	0.50	82.1
298	Blank	1.8	—	—	—	930	151.1	0.77	—
	5×10^{-6}	1.7	22.3	15.4	0.95	2606	81.5	0.57	64.3
	10^{-5}	2.7	23.1	6.3	1.00	4985	48.3	0.62	81.3
	3.2×10^{-5}	1.5	26.6	5.0	0.87	16 330	74.9	0.51	94.3
	10^{-4}	2.2	13.4	7.1	1.00	22 020	63.9	0.56	95.8
308	Blank	1.9	—	—	—	516.5	82.8	0.87	—
	5×10^{-6}	1.7	666.1	24.6	0.85	2382	95.4	0.69	78.3
	10^{-5}	2.4	24.4	9.7	0.84	5406	126.3	0.47	90.4
	3.2×10^{-5}	2.6	1020	14.2	0.80	6415	72.7	0.59	91.9
	10^{-4}	2.0	1251	9.0	0.80	12 600	58.2	0.47	95.9
318	Blank	1.6	—	—	—	483.6	131.5	0.82	—
	5×10^{-6}	1.9	321.2	24.5	0.88	703.4	236.6	0.61	31.2
	10^{-5}	1.6	4.5	85.9	0.50	2753	107.6	0.90	82.4
	3.2×10^{-5}	2.8	835.5	9.7	0.82	6036	52.0	0.59	92.0
	10^{-4}	2.3	1228	11.1	0.80	10 120	63.8	0.54	95.2

The circuit model provides a kind of effective quantitative analysis method for the electrical parameters of the metal/solution interfaces and the evaluation of the AC impedance value is illustrated in Table 2. It can be seen from Table 2 that the change in the concentration of prothioconazole from 5×10^{-6} to 10^{-4} M leads to variation of the inhibition efficiency from 64.3% to

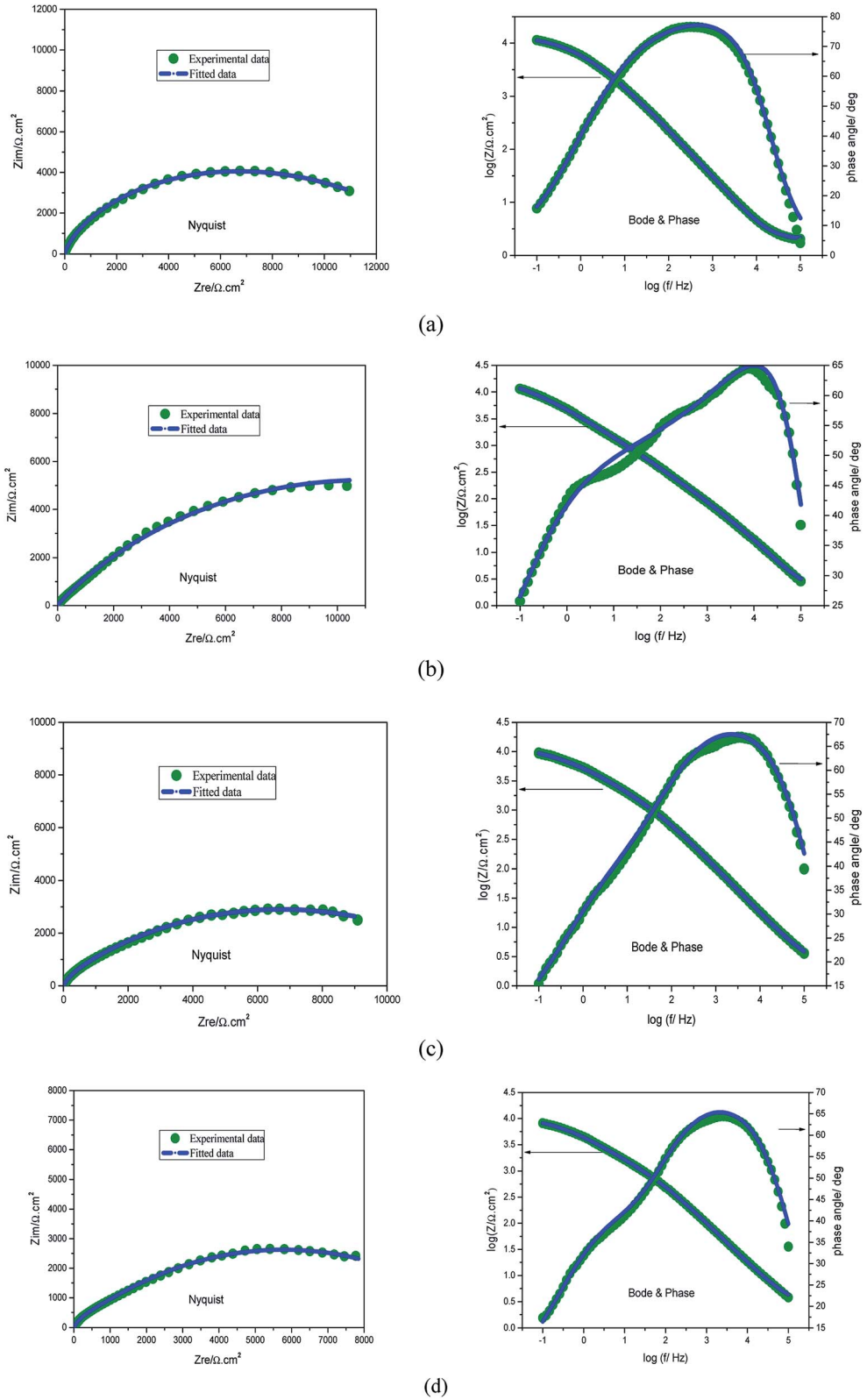

Fig. 5 Fitting analysis of the Nyquist and Bode plots for copper in acidic solution with 10^{-4} M prothioconazole at different temperatures: (a) 288; (b) 298; (c) 308; and (d) 318 K.

95.8% correspondingly at 298 K, while the Y_f values tended to decrease in the presence of the prothioconazole, in part this is probably due to prothioconazole gradually replacing the water molecules in the active adsorption point of the Cu surface.[30] The R_{ct} values increased with the increasing concentration of prothioconazole revealing that the charge transfer reactions may take place on the sites of dissociative adsorption of the electrode/electrolyte interface.[31] When the prothioconazole concentration reached 10^{-4} M, more inhibitor molecules adsorb onto the Cu surface, and corrosion inhibitor efficiencies of up to 82.1%, 95.8%, 95.9% and 95.2% were recorded for 288, 298, 308 and 318 K, respectively. Furthermore, Bode and phase plots were extracted by adopting the equivalent circuit (R(Q(R(QR)))) based on the curve fitting. As Fig. 5 shows, the degree of fitting is high. The order of the anticorrosion ability of prothioconazole has a similar trend to the data obtained from the EIS and Tafel testing.

3.3. Adsorption isotherms

In general, two models of physical adsorption and chemisorption might be involved during the adsorption of the organic compound on the electrode surface and the adsorption behaviors markedly improve the anti-corrosion capacity of the metals. The adsorption model is an effective analysis tool for explaining the anticorrosive mechanism,[32] therefore, this paper focuses on the static equilibrium adsorption behaviors and the confirmation of the adsorption characteristics. The fractional surface coverage (θ) was acquired from the corresponding EIS test for different prothioconazole concentrations and temperatures in acidic solutions, the value of θ was described using the expression:[33]

$$\theta = \frac{R_{ct} - R_{ct}^0}{R_{ct}} \quad (5)$$

To provide detailed molecular adsorption information for the prothioconazole and metal surface, general models of liquid/metal phase adsorption were tested as follows:

Frumkin isotherm:[34,35]

$$KC = \frac{\theta}{X(1-\theta)^X} \exp(-2a\theta) \quad (6)$$

Bockris–Swinkels isotherm:[36]

$$KC = \frac{\theta}{(1-\theta)^X} \frac{[X(1-\theta)+\theta]^{(X-1)}}{X^X} \quad (7)$$

Damaskin–Parsons isotherm:[37]

$$KC = \frac{\theta}{(1-\theta)^X} \exp(-f\theta) \quad (8)$$

Kastening–Holleck isotherm:[38]

$$KC = \left(1 - \theta + \frac{\theta}{X}\right)^{(X-1)} \frac{\theta}{X(1-\theta)^X} \exp(-f\theta) \quad (9)$$

Flory–Huggins isotherm:[39]

$$KC = \frac{\theta/X}{(1-\theta)^X} \quad (10)$$

Dhar–Flory–Huggins isotherm:[39]

$$KC = \frac{\theta}{\exp(X-1)(1-\theta)^X} \quad (11)$$

Table 3 The adsorption isotherm model fitting parameters for copper in acidic solution at different temperatures

Temperature (K)	Isotherm model	Correlation coefficient (R^2)	K (L mol^{-1})	X	ΔG_{ads}^0 (kJ mol^{-1})
288	Frumkin	0.97528	2.19×10^5	3.4	−39.06
	Bockris–Swinkels	0.98707	1.21×10^5	4.7	−37.64
	Kastening–Holleck	0.98027	7.54×10^8	0.3	−58.56
	Flory–Huggins	0.98781	4.94×10^5	3.0	−41.01
	Dhar–Flory–Huggins	0.98781	1.97×10^5	3.0	−38.81
	Langmuir	0.99862	1.99×10^5	1.0	−38.84
298	Bockris–Swinkels	0.9704	1.69×10^7	3.9	−51.18
	Flory–Huggins	0.96932	2.52×10^8	3.6	−57.88
	Dhar–Flory–Huggins	0.96932	6.67×10^7	3.6	−54.59
	Langmuir	0.99976	4.67×10^5	1.0	−42.29
308	Bockris–Swinkels	0.97118	1.50×10^6	2.0	−46.70
	Flory–Huggins	0.97133	2.48×10^6	1.9	−47.98
	Dhar–Flory–Huggins	0.97133	1.87×10^6	1.9	−47.27
	Langmuir	0.99985	7.94×10^5	1.0	−45.07
318	Frumkin	0.99769	4.97×10^3	2.6	−33.12
	Bockris–Swinkels	0.98957	1.30×10^6	2.1	−47.84
	Damaskin–Parsons	0.99769	1.30×10^4	2.6	−35.65
	Kastening–Holleck	0.99807	5.54×10^3	2.7	−33.41
	Flory–Huggins	0.98881	2.32×10^6	2.0	−49.36
	Dhar–Flory–Huggins	0.98881	1.67×10^6	2.0	−48.50
	Langmuir	0.98733	1.70×10^5	1.0	−42.46

and the Langmuir isotherm:[40]

$$KC = \frac{\theta}{1-\theta} \quad (12)$$

in which C represents the prothioconazole concentration, K represents the adsorption equilibrium constant and X represents the number of water molecules displaced by one prothioconazole inhibitor molecule. α is the parameter of interaction between the molecules adsorbed on the metal surface. The most common main fitting parameters such as K, X and the fitting correlation coefficient (R^2) were analyzed and the data are shown in Table 3. Typically, the best-fitting isotherm equation was determined by the fitting value of R^2. The results showed that the Langmuir and Bockris–Swinkels isotherms provide a better description of the adsorption behavior of prothioconazole on the surface of the metal, and the Langmuir isotherm assumes that all adsorption sites are equivalent. The linear fitting curve for the adsorption of prothioconazole on the metal surface was obtained to show the relationship between C/θ and C, and is shown in Fig. 6a. On the other hand, the nonlinear least square fit to the θ base in the Bockris–Swinkels isotherms at different temperatures are shown in Fig. 6b. The nonlinear fitting method was applied to calculate the number X which represented the number of water molecules. A value of X equal to 2.0 indicates that one molecule of prothioconazole substitutes two molecules of water that were first adsorbed on the metal surface. The fitting parameters of some of the empirical adsorption models are also listed in Table 3, it can be observed that the number of substituted water molecules decreased from 4.7 to 2.0 with the increasing experimentation temperature based on using the Bockris–Swinkels isothermal model to fit the data, in other words, the sorption capacities of prothioconazole decreased with the increase in the molecular hot movement strength.[41] Meanwhile the inhibitor molecule should maintain the balance of adsorption–desorption on the metal, however, the homeostasis of the water molecule desorption and the prothioconazole adsorption has been broken owing to the enhancement of the molecular hot movement with the rise in temperature; as a result, X has a decreasing trend. According to Table 3, all of the values of R^2 for the Langmuir isotherm exceeded 0.987, indicating that the isotherm models fit our experimental data well. Generally, the adsorption equilibrium constant (K) was related to the free energy of adsorption ΔG^0_{ads} as follows:[41,42]

$$K = \frac{1}{C_{solvent}} \exp\left(-\Delta G^0_{ads}/RT\right) \quad (13)$$

In which $C_{solvent}$ is the molar concentration of the water solvent, which takes the value of 55.5 mol L^{-1}. T is the thermodynamic temperature and R represents the molar gas constant. The thermodynamic parameters $\Delta G^0_{ads}$for the adsorption process of prothioconazole obtained from the most commonly used adsorption isotherms mentioned above are also presented in Table 3. Generally, the larger the value of K and the more negative the value of ΔG^0_{ads},the stronger the coherence of the studied inhibitor to the metal surface.[43,44] Furthermore, the values of ΔG^0_{ads} that are less than -40 kJ mol^{-1} demonstrate that the metal surface adsorbed the studied organic compound mainly *via* chemical adsorption.[44] It was found from Table 3 that prothioconazole displayed a larger value of K and the valid values for the ΔG^0_{ads} parameter range from -33.1 to -58.6 kJ mol^{-1} indicating that the prothioconazole possessed a stronger adsorption ability and the adsorption was a spontaneous process.[45] Furthermore, the results of the free energy of adsorption show that prothioconazole has a good chemisorption that involves either transferring or sharing electrons to form a coordinate type of bond.[46,47] From Table 3 it can also be found that the ΔG^0_{ads} showed a very slight variation with an increase in the temperature based on the Langmuir isothermal model to fit the data. Theoretically, the chemisorption process of the inhibitor on metal surface is highly stable, even at 318 K, and this could be attributed to its strong adsorptive action rather than a physisorption process.[48]

3.4. SEM analysis and weight loss tests

Fig. 7 presents the SEM apparent morphology of the metal surface modified by 10^{-4} M prothioconazole exposed to 0.5 M

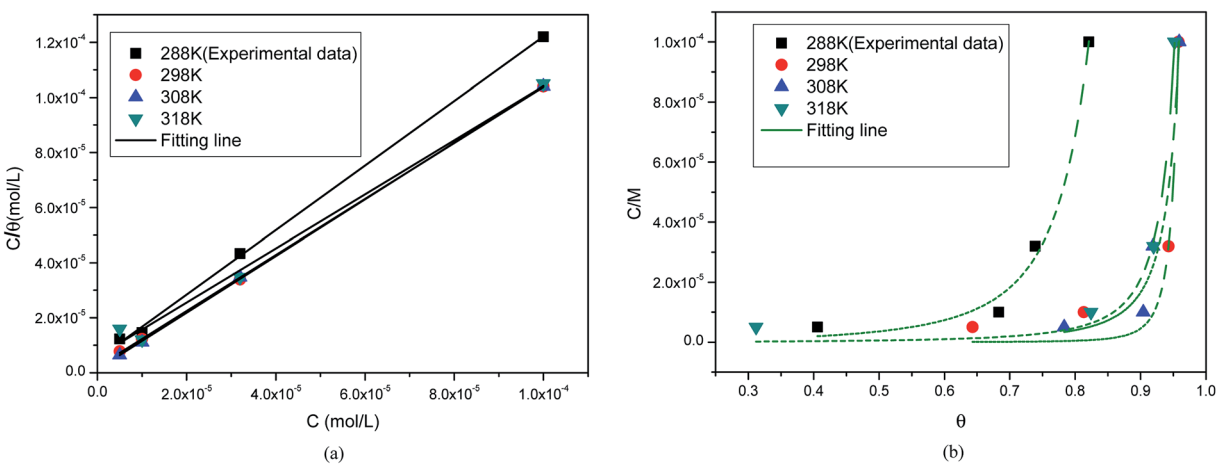

Fig. 6 Points representing the values of the average surface coverage (θ) as a function of C for copper in 0.5 M H_2SO_4 at different temperatures: (a) Langmuir isothermal model; and (b) Bockris–Swinkels model.

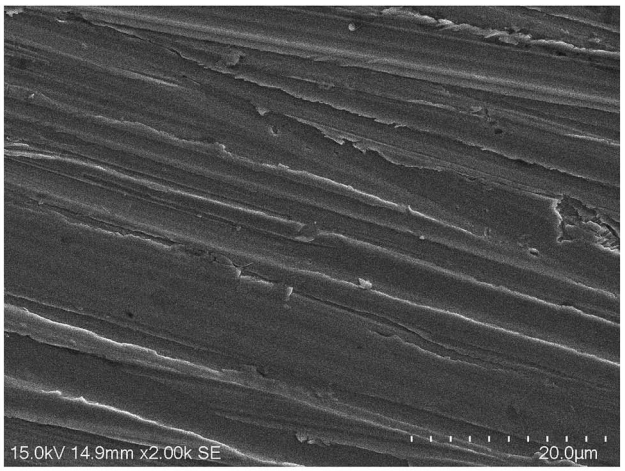

(a)

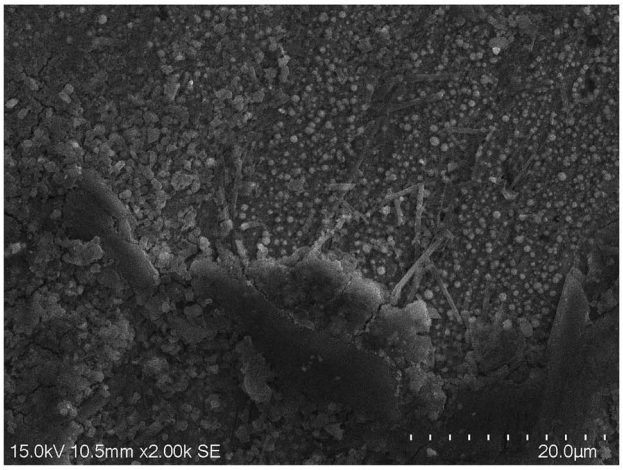

(b)

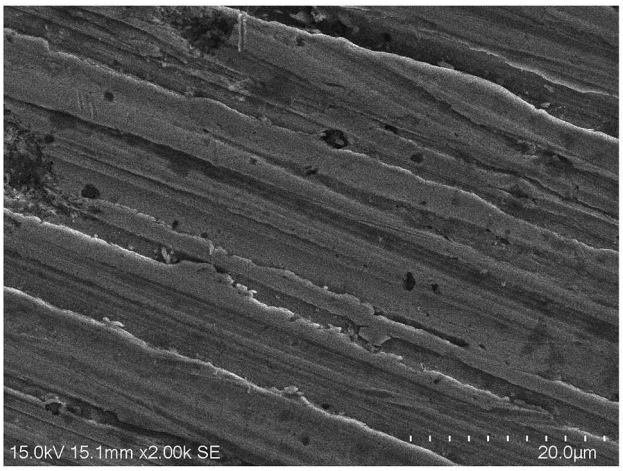

(c)

Fig. 7 SEM morphology of copper samples (a) after surface polishing only, (b) after being immersed in 0.5 M H_2SO_4 for 8 h at 308 K, and (c) after immersion in 0.5 M H_2SO_4 with 10^{-4} M prothioconazole.

H_2SO_4 solution for 8 h at 308 K. Before immersion in the acidic solution, a mechanical polishing treatment of the sample surface was performed to provide a freshly polished metal surface (Fig. 7a). The copper surface suffered corrosion damage and presented small cracks for the etching solution in the absence of the prothioconazole inhibitor (Fig. 7b). After the 10^{-4} M prothioconazole inhibitor was added to the solution, significantly less damage occurred on the metal surface and the original polishing scratches are clearly visible in Fig. 7c. Thus, it is inferred that the corrosion reaction rate of the metal was inhibited when prothioconazole was added to the solution and the studied inhibitor provided a good anticorrosion performance for the Cu metal.

The corrosion behavior of Cu in 0.5 M H_2SO_4 solution was investigated using the weight loss method. The values of the corrosion rate (W) were obtained using the following equation:

$$W = \frac{m_1 - m_2}{S \times t} \tag{14}$$

The symbol m_1 represents the mass of copper metal before corrosion and m_2 is the mass of copper metal after corrosion. S represents the surface area of the copper block and t represents the corrosion time.

$$S = 2(lw + lh + wh) \tag{15}$$

In which l is the length, w is the width, and h is the height. The corrosion rate (W) can be calculated in the weight loss experiment and its unit is mg $(cm^2\ h)^{-1}$. Therefore the inhibition efficiency of weight loss is obtained from the following equation:

$$\eta_w\% = \frac{W_0 - W}{W_0} \times 100 \tag{16}$$

W is the copper corrosion rate with the inhibitor in acidic medium, W_0 represents the corrosion rate without the inhibitor prothioconazole in 0.5 M H_2SO_4 solution.

The preservative properties obtained from different concentrations of prothioconazole in acidic solution are given in Table 4. The corrosion weight loss decreased gradually with the increasing concentration of the prothioconazole compound, leading to an increase of the η_w (inhibition efficiencies) up to 87.6% for 308 K. Therefore, it is worth mentioning that prothioconazole represents a better inhibitive ability.

3.5. Molecular modeling

The relationship between the prothioconazole molecular structure and the properties of anticorrosion was discussed using quantum chemical calculations and frontier molecular orbitals (FMO) theory in this paper.[49] The optimized geometric structures such as LUMO (the lowest unoccupied molecular orbital), and HOMO (the highest occupied molecular orbital) density distribution of prothioconazole are revealed in Fig. 8. It can be observed that the FMO distribution of the prothioconazole molecule are grouped in the triazole and benzene rings, and the –C═S atoms, which could be directly involved in the higher electron cloud density region.[50] The frontier orbital system represents a potential active adsorption point for the triazole/benzene rings and the –C═S atoms. It is usually

Table 4 Weight loss analysis for copper in acidic solution with different concentrations of prothioconazole at 308 K

C (M)	S (cm^2)	m (mg)	W (mg cm^{-2} h^{-1})	η_w%
Blank	10.75	3.8	0.04419	—
5.0×10^{-6}	11.39	2.5	0.02744	37.9
1.0×10^{-5}	11.71	1.9	0.02028	54.1
3.2×10^{-5}	9.58	1.0	0.01305	70.5
1.0×10^{-4}	11.37	0.5	0.005497	87.6

considered that the higher the energy of E_{HOMO}, the stronger its corresponding electron-donating ability, therefore leading to the electron easily moving into an empty molecular orbital. Although a smaller value of E_{LUMO} represents a strong electron-receiving ability and a lower value of ΔE ($\Delta E = E_{LUMO} - E_{HOMO}$) is an index of the strong adsorption tendency to the metal surface.[51]

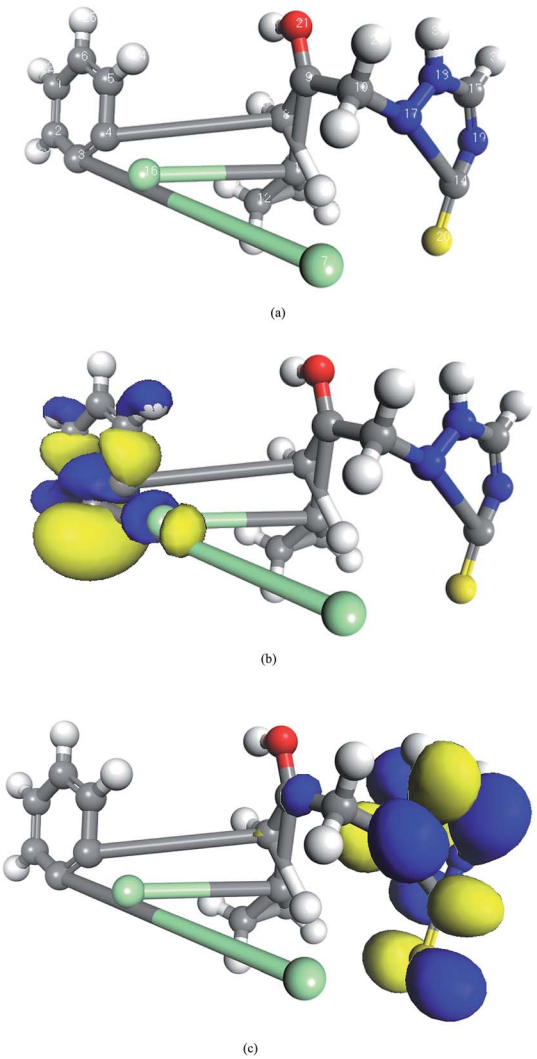

Fig. 8 The frontier orbital density distributions of prothioconazole in the aqueous phase: (a) optimized structure; (b) HOMO, $E_{HOMO} = -4.857$ eV; and (c) LUMO, $E_{LUMO} = -3.941$ eV.

Fukui functions can be used to provide nucleophilic electrophilic reaction data for determining the reaction activity site.[51] Generally, the Fukui function f is related to the finite-difference approximation as follows:[52]

$$\text{For an electrophilic attack, } f^- = q(N) - q(N-1) \quad (17)$$

$$\text{For a nucleophilic attack, } f^+ = q(N+1) - q(N) \quad (18)$$

In which, $q(N)$, $q(N+1)$ and $q(N-1)$ represent the charges of the neutral, cationic and anionic states, respectively. The specification of the Fukui function can be further defined as follows:[53]

$$\Delta f = f^+ - f^- \quad (19)$$

In general, $\Delta f > 0$ signifies the reactive site tends towards a nucleophilic attack, while $\Delta f < 0$ implies an electrophilic attack.[52] The condensed Fukui functions obtained using the GGA/BLYP method with geometrical optimization are given in Table 5. Based on the results obtained from Table 5, it is observed that the reaction active areas of prothioconazole are

Table 5 The condensed Fukui functions for the prothioconazole molecule

Atom	f^+	f^-	Δf
C(1)	0.022	0.023	−0.001
C(2)	0.024	0.025	−0.001
C(3)	0.093	0.090	0.003
C(4)	0.019	0.020	−0.001
C(5)	0.018	0.018	0
C(6)	0.018	0.019	−0.001
Cl(7)	0.147	0.171	−0.024
C(8)	0.036	0.035	0.001
C(9)	0.031	0.032	−0.001
C(10)	0.014	0.012	0.002
C(11)	0.011	0.011	0
C(12)	0.015	0.018	−0.003
C(13)	0.021	0.023	−0.002
C(14)	0.025	0.023	0.002
C(15)	0.048	0.050	−0.002
Cl(16)	0.049	0.028	0.021
N(17)	0.046	0.035	0.011
N(18)	0.021	0.019	0.002
N(19)	0.025	0.027	−0.002
S(20)	0.081	0.077	0.004
O(21)	0.036	0.039	−0.003
H(22)	0.014	0.014	0
H(23)	0.018	0.018	0
H(24)	0.013	0.013	0
H(25)	0.011	0.011	0
H(26)	0.017	0.017	0
H(27)	0.006	0.004	0.002
H(28)	0.012	0.011	0.001
H(29)	0.016	0.015	0.001
H(30)	0.007	0.012	−0.005
H(31)	0.013	0.012	0.001
H(32)	0.012	0.014	−0.002
H(33)	0.012	0.014	−0.002
H(34)	0.019	0.019	0
H(35)	0.014	0.013	0.001
H(36)	0.015	0.014	0.001

distributed on the triazole/benzene rings and its polar functional groups.

The nitrogen atom of N3 on the benzene ring take on the maximum value of $f^-$and the nucleophilic centers can obtain electrons from the metal surface, thus forming a back-donating bond. From Table 5, it can also be observed that the triazole ring and polar functional groups were electrophilic reactive centers, which can provide electrons to the Cu surface and form a coordinate bond. Comparison with the results shown in Table 5 and Fig. 8 indicates that this method using the Fukui functions and FMO is in good agreement with the prediction of the active sites for adsorption and the mechanism for gaining (losing) an electron from prothioconazole.[54]

4. Conclusions

This study presented a novel efficient organic anti-corrosion compound for copper in 0.5 M H_2SO_4 solution based on propanthiazole, which has better biological activity, no teratogenicity and is safer for humans and the environment compared to the existing method. The results obtained led to the following conclusions:

(i) Prothioconazole was demonstrated to be an effective corrosion inhibitor for Cu metal in acidic media, and the inhibition effects obtained from all the electrochemical measurements were in good agreement. The inhibition efficiency increased with increasing prothioconazole concentration under the conditions of constant temperature.

(ii) The adsorption isotherm experiments displayed a larger value of K, and the valid values for the ΔG^0_{ads} parameter ranged from -33.1 to -58.6 kJ mol^{-1}; this indicated that chemisorption coexists in the modification process and that adsorption was a spontaneous process.

(iii) SEM and weight loss testing indicated that the corrosion of the copper block was inhibited when prothioconazole was added to the corrosion solution. Molecular modeling showed that the triazole and benzene rings and the –C=S atoms were the main active sites for the adsorption process.

Conflicts of interest

There are no conflicts to declare.

Acknowledgements

The authors gratefully acknowledge the support of Sichuan Science and Technology Program (2019YFG0101, 2019YFG0280), the Key Science and Technology Project of Sichuan Province (2019ZDZX0026), the National Natural Science Foundation of China (No. 61841401), and the Dongguan Entrepreneurial Talent Program.

References

1 D. Kong, A. Xu and C. Dong, Electrochemical investigation and ab initio computation of passivefilm properties on copper in anaerobic sulphide solutions, *Corros. Sci.*, 2017, **116**, 34–43.
2 H. Yu, C. Li, B. Yuan, L. Li and C. Wang, The inhibitive effects of AC-treated mixed selfassembled monolayers on copper corrosion, *Corros. Sci.*, 2017, **120**, 231–238.
3 A. I. Ikeuba, B. Zhang, J. Wang, E.-H. Han and W. Ke, Electrochemical, TOF-SIMS and XPS studies on the corrosion behavior of Q-phase in NaCl solutions as a function of pH, *Appl. Surf. Sci.*, 2019, **490**, 535–545.
4 F. Li, S. Zhang, Y. Lu, B. Tan, S. Chen and L. Guo, Synergistic corrosion inhibition effect of thiazolyl-based ionic liquids between anions and cations for copper in HCl solution, *Appl. Surf. Sci.*, 2019, **483**, 901–911.
5 H. Gerengi, M. Mielniczek, G. Gece and M. M. Solomon, Experimental and Quantum Chemical Evaluation of 8-Hydroxyquinoline as a Corrosion Inhibitor for Copper in 0.1 M HCl, *Ind. Eng. Chem. Res.*, 2016, **55**, 9614–9624.
6 N. Kovačević, I. Milošev and A. Kokalj, How relevant is the adsorption bonding of imidazoles and triazoles for their corrosion inhibition of copper?, *Corros. Sci.*, 2017, **124**, 25–34.
7 D. Kong, A. Xu and C. Dong, Electrochemical investigation and ab initio computation of passivefilm properties on copper in anaerobic sulphide solutions, *Corros. Sci.*, 2017, **116**, 34–43.
8 N. D. Nam, V. Q. Thang, N. T. Hoai and P. V. Hien, Yttrium 3-(4-nitrophenyl)-2-propenoate used as inhibitor against copper alloy corrosion in 0. 1 M NaCl solution, *Corros. Sci.*, 2016, **112**, 451–461.
9 Z. Tao, W. He, S. Wang, X. He, C. Jiao and D. Xiao, Synergistic effect of different additives on microvia filling in an acidic copper plating solution, *J. Electrochem. Soc.*, 2016, **163**, 379–384.
10 I. B. Obota, D. D. Macdonald and Z. M. Gasem, Density functional theory (DFT) as a powerful tool for designing new organic corrosion inhibitors. Part 1: an overview, *Corros. Sci.*, 2015, **99**, 1–30.
11 Y. Qiang, S. Zhang, L. Guo, X. Zheng, B. Xiang and S. Chen, Experimental and theoretical studies of four allyl imidazolium-basedionic liquids as green inhibitors for copper corrosion in sulfuric acid, *Corros. Sci.*, 2017, **119**, 68–78.
12 H. Tian, W. Li and B. Hou, Novel application of a hormone biosynthetic inhibitorfor the corrosion resistance enhancement of copper in synthetic seawater, *Corros. Sci.*, 2011, **539**, 3435–3445.
13 Z. Tao, G. Liu, Y. Li, R. Zhang and H. Su, Electrochemical investigation of tetrazolium violet as a novel copper corrosion inhibitor in an acid environment, *ACS Omega*, 2020, **5**, 4415–4423.
14 S. Zhang, Z. Tao, W. Li and B. Hou, Substitutional adsorption isotherms and corrosion inhibitive properties of some oxadiazol–triazole derivative in acidic solution, *Corros. Sci.*, 2010, **52**, 3126–3132.
15 T. T. Qin, J. Li, H. Q. Luo, M. Li and N. B. Li, Corrosion inhibition of copper by 2,5-dimercapto-1,3,4-thiadiazole

monolayer in acidic solution, *Corros. Sci.*, 2011, **53**, 1072–1078.

16 Y. Gong, Z. Wang, F. Gao, S. Zhang and H. Li, Synthesis of new benzotriazole derivatives containing carbon chains as the corrosion inhibitors for copper in sodium chloride solution, *Ind. Eng. Chem. Res.*, 2015, **54**, 12242–12253.

17 Sudheer and M. A. Quraishi, Electrochemical and theoretical investigation of triazole derivatives on corrosion inhibition behavior of copper in hydrochloricacid medium, *Corros. Sci.*, 2013, **30**, 161–169.

18 M. Mousavi and T. Baghgoli, Application of interaction energy in quantitativestructure-inhibition relationship study of some benzenethiol derivatives oncopper corrosion, *Corros. Sci.*, 2016, **105**, 170–176.

19 M. Finšgar, EQCM and XPS analysis of 1,2,4-triazole and 3-amino-1,2,4-triazole as copper corrosion inhibitors in chloride solution, *Corros. Sci.*, 2013, **77**, 350–359.

20 A. K. Satapathy, G. Gunasekaran, S. C. Sahoo, K. Amit and P. V. Rodrigues, Corrosion inhibition by *Justicia gendarussa* plant extract in hydrochloric acid solution, *Corros. Sci.*, 2009, **51**, 2848–2856.

21 J. Wang, Inhibitor-concentration-induced extreme behaviour in electrochemical parameters, *Chin. J. Oceanol. Limnol.*, 1998, **16**, 183–188.

22 X. Zheng, S. Zhang, W. Li, M. Gong and L. Yin, Experimental and theoretical studiesof two imidazolium-based ionic liquids as inhibitors for mild steel in sulfuricacid solution, *Corros. Sci.*, 2015, **95**, 168–179.

23 L. Hu, S. Zhang, W. Li and B. Hou, Electrochemical and thermodynamicinvestigation of diniconazole and triadimefon as corrosion inhibitors forcopper in synthetic seawater, *Corros. Sci.*, 2010, **52**, 2891–2896.

24 Z. Khiati, A. A. Othman, M. Sanchez-Moreno, M. C. Bernard, S. Joiret, E. M. M. Sutter and V. Vivier, Corrosion inhibition of copper in neutral chloride media by anovel derivative of 1,2,4-triazole, *Corros. Sci.*, 2011, **53**, 3092–3099.

25 K. M. Ismail, Evaluation of cysteine as environmentally friendly corrosion inhibitor for copper in neutral and acidic chloride solutions, *Electrochim. Acta*, 2007, **52**, 7811–7819.

26 G. Žerjav and I. Milošev, Protection of copper against corrosion insimulated urban rain by the combined action of benzotriazole, 2-mercaptobenzimidazole and stearic acid, *Corros. Sci.*, 2015, **98**, 180–191.

27 Z. Ghelichkhah, S. Sharifi-Asl, K. Farhadi, S. Banisaied, S. Ahmadi and D. D. Macdonald, L-Cysteine/polydopamine nanoparticle-coatings for copper corrosion protection, *Corros. Sci.*, 2015, **91**, 129–139.

28 X. Zhang, Q. Liao, K. Nie, L. Zhao, D. Yang, Z. Yue, H. Ge and Y. Li, Self-assembled monolayers formed by ammonium pyrrolidine dithiocarbamate on copper surfaces in sodium chloride solution, *Corros. Sci.*, 2015, **93**, 201–210.

29 H. Wei, Y. Wei, L. Hou and N. Dang, Correlation of ageing precipitates with the corrosion behaviour of Cu–4 wt% Ti alloys in 3.5 wt% NaCl solution, *Corros. Sci.*, 2016, **111**, 382–390.

30 Z. Tao, W. He, S. Wang and G. Zhou, Electrochemical study of cyproconazole as a novel corrosion inhibitor for copper in acidic solution, *Ind. Eng. Chem. Res.*, 2013, **52**, 17891–17899.

31 A. Singh, K. R. Ansari, J. Haque, P. Dohare, H. Lgaz, R. Salghi and M. A. Quraishi, Effect of electron donating functional groups on corrosion inhibition of mild steel in hydrochloric acid: experimental and quantum chemical study, *J. Taiwan Inst. Chem. Eng.*, 2018, **82**, 233–251.

32 R. Solmaz, E. A. Sahin, A. Doner and G. Kardas, The investigation of synergistic inhibition effect of rhodanine and iodide ion on the corrosion of copper in sulphuric acid solution, *Corros. Sci.*, 2011, **53**, 3231–3240.

33 L. C. Murulana, M. M. Kabanda and E. E. Ebenso, Investigation of the adsorption characteristics of some selected sulphonamide derivatives as corrosion inhibitors at mild steel/hydrochloric acid interface: experimental, quantum chemical and QSAR studies, *J. Mol. Liq.*, 2016, **215**, 763–779.

34 D. D. Do, *Adsorption Analysis: Equilibria and Kinetics*, Imperial College Press, London, 1998, DOI: 10.1142/9781860943829.

35 K. Anton, D. Gustinčič, M. Poberžnik and M. Lozinšek, New insights into adsorption bonding of imidazole: a viable C_2–H bond cleavage on copper surfaces, *Appl. Surf. Sci.*, 2019, **479**, 463–468.

36 J. O. Bockris and D. A. J. Swinkels, Adsorption of *n*-decylamine on solid metal electrodes, *J. Electrochem. Soc.*, 1964, **111**, 736.

37 B. B. Damaskin, O. A. Petrii, V. V. Batrakov, in *Adsorption of Organic Compounds on Electrodes*, Plenum Press, New York, 1971, pp. 86, 94, 247, DOI: 10.1149/1.2404464.

38 B. Kastening and L. Holleck, Die bedeutung der adsorption in der polarographie, *Talanta*, 1965, **12**, 1259–1288.

39 H. P. Dhar, B. E. Conway and K. M. Joshi, On the form of adsorption isotherms for substitutional adsorption of molecules of different sizes, *Electrochim. Acta*, 1973, **18**, 789–798.

40 I. Langmuir, The adsorption of gases on plane surfaces of glass, mica and platinum, *J. Am. Chem. Soc.*, 1918, **40**, 1361–1403.

41 *Adsorption of Molecules at Metal Electrodes*, ed. J. Lipowski and P. N. Ross, VCH, Weinheim, New York, 1992, ISBN 3-527-28008-1, DOI: 10.1002/bbpc.19920961247.

42 M. A. Amin, Q. Mohsen and O. A. Hazzazi, Synergistic effect of I – ions on the corrosion inhibition of Al in 1.0 M phosphoric acid solutions by purine, *Mater. Chem. Phys.*, 2009, **114**, 908–914.

43 N. O. Obi-Egbedi and I. B. Obot, Inhibitive properties, thermodynamic and quantum chemical studies of alloxazine on mild steel corrosion in H_2SO_4, *Corros. Sci.*, 2011, **53**, 263–275.

44 A. Döner, A. O. Yüce and G. Kardaş, Inhibition effect of rhodanine-*N*-acetic acid on copper corrosion in acidic media, *Ind. Eng. Chem. Res.*, 2013, **52**, 9709–9718.

45 V. Srivastava, J. Haque, C. Verma, P. Singh, H. Lgaz, R. Salghi and M. A. Quraishi, Amino acid based imidazolium zwitterions as novel and green corrosion inhibitors for

mild steel: experimental, DFT and MD studies, *J. Mol. Liq.*, 2017, **244**, 340–352.

46 Z. Szklarska-Smialowska and J. Mankowski, Crevice corrosion of stainless steels in sodium chloride solution, *Corros. Sci.*, 1978, **18**, 953.

47 A. Yurt, S. Ulutas and H. Dal, Electrochemical and theoretical investigation on the corrosion of aluminium in acidic solution containing some Schiff bases, *Appl. Surf. Sci.*, 2006, **253**, 919–925.

48 Y. Wang, Z. Liu, D. Li, Y. Dong, W. Li and N. Li, The polymeric nanofilm of triazinedithiolsilane fabricated by self-assembled technique on copper surface. Part 1: design route and corrosion resistance, *Corros. Sci.*, 2015, **98**, 382–390.

49 A. Dutta, S. K. Saha, U. Adhikari, P. Banerjee and D. Sukul, Effect of substitution on corrosion inhibition properties of 2-(substituted phenyl) benzimidazole derivatives on mild steel in 1 M HCl solution: a combined experimental and theoretical approach, *Corros. Sci.*, 2017, **123**, 256–266.

50 C. Jing, Z. Wang, Y. Gong, H. Huang, Y. Ma, H. Xie, H. Li, S. Zhang and F. Gao, Photo and thermally stable branched corrosion inhibitors containing two benzotriazole groups for copper in 3.5 wt% sodium chloride solution, *Corros. Sci.*, 2018, **138**, 353–371.

51 H. M. Abd El-Lateef, M. A. Abo-Riya and A. H. Tantawy, Empirical and quantum chemical studies on the corrosion inhibition performance of some novel synthesized cationic gemini surfactants on carbon steel pipelines in acid pickling processes, *Corros. Sci.*, 2016, **108**, 94–110.

52 L. Guo, W. Dong and S. Zhang, Theoretical challenges in understanding the inhibition mechanism of copper corrosion in acid media in the presence of three triazole derivatives, *RSC Adv.*, 2014, **4**, 41956–41967.

53 Y. Liu, S. Li, J. Zhang, J. Liu, Z. Han and L. Ren, Corrosion inhibition of biomimetic super-hydrophobic electrodeposition coatings on copper substrate, *Corros. Sci.*, 2015, **94**, 190–196.

54 A. Kokalj, Is the analysis of molecular electronic structure of corrosion inhibitors sufficient to predict the trend of their inhibition performance, *Electrochim. Acta*, 2010, **56**, 745–755.